Proc. Indian Acad. Sci. **A55** 131–152 (1962)

The vibration spectrum of lithium fluoride and the evaluation of its specific heat

SIR C V RAMAN
Memoir No. 130 of the Raman Research Institute, Bangalore-6

Received March 6, 1962

1. Introduction

Lithium fluoride crystallises in the cubic system, the crystal structure being similar to that of rock-salt and it also exhibits similar cleavage properties. But in other respects, lithium fluoride differs markedly from rock-salt. Though the atomic weights of both the component elements in lithium fluoride are much smaller, its density is substantially greater than that of rock-salt, being 2·60 as against 2·17. The solubility of lithium fluoride in water is also extremely low. It is clear from these facts that the binding between the metal and halogen atoms is far stronger in lithium fluoride than in rock-salt. Hence the strength of such binding would be quite as important a factor as the lower atomic weights in determining the spectroscopic behaviour of lithium fluoride.

In Memoirs Nos. 127, 128 and 129 of this Institute published in these *Proceedings* in recent months, the author has described studies on the infra-red behaviour of three crystals of simple structure and composition, viz., MgO, NaCl and diamond and shown that the results enable us to determine the characteristic modes and frequencies of free vibration of the atomic nuclei in their structures. It was further shown that on the basis of the spectroscopically determined frequencies and without making use of any other data, it is possible to evaluate the thermal energy of the crystals as a function of the temperature over the entire range extending from the absolute zero upwards up to that at which the specific heat reaches its limiting value. The present memoir aims to accomplish this also in the case of lithium fluoride.

2. The free vibrations of the structure

We may usefully begin by recapitulating briefly the considerations of the same nature as those set out and discussed in much greater detail in the memoirs on MgO and NaCl referred to above. The dispersion, absorption and reflection of

infra-red radiation by a crystal are effects arising from the interaction of the electromagnetic field in the radiation with the structural units forming the crystal. As a first step towards the understanding of these effects, it is necessary to consider the nature of the spectrum of the free or spontaneous vibrations of these structural units. We may deduce their modes and frequencies by the methods of classical mechanics. For this purpose the atomic nuclei may be regarded as simple mass particles and the electronic clouds surrounding them as massless springs which hold the structure together.

It emerges that the vibrational mode of highest frequency of the lithium fluoride structure is one in which the nuclei of lithium and fluorine oscillate against each other in opposite phases. Eight other modes of free vibration are also possible. They may be described very simply in terms of the crystal structure. Four of the modes are oscillations of the cubic layers, while the four other modes are the oscillations of the octahedral layers, the movements alternating in phase from layer to layer and being either normal or tangential to those layers. Since the oscillations of the lithium and fluorine nuclei may be either in the same phase or in opposite phases, we have four modes of the cubic layers and four modes of the octahedral layers and hence eight in all. The oscillations of lithium and fluorine nuclei located in the same cubic layers would be coupled with each other and hence would both appear in each of the four modes under reference. But since the lithium and fluorine nuclei appear in distinct layers parallel to the octahedral planes, their oscillations would be independent. In other words, only the layers containing the lithium nuclei would oscillate in two of the modes, the movements being respectively normal and tangential to the layers. Likewise, only the layers containing the fluorine nuclei would oscillate in the two other modes.

3. The vibrational frequencies

The forces which determine the frequencies of vibration in each of the nine modes arise from the displacements relative to an oscillating nucleus of the other nuclei in its neighbourhood. In a first approximation, it is sufficient to consider the interactions between each nucleus and its six immediate neighbours. A special feature of the present case is the great disparity between the atomic weights of lithium and fluorine, which are 6·94 and 19 respectively. Important consequences result from this disparity. The modes in which the lithium nuclei alone oscillate would have notably higher frequencies than those in which the fluorine nuclei alone oscillate. As a further consequence, we should find that the coupled vibrations of the nuclei located in the cubic layers would similarly separate into two pairs, one with higher and the other with lower frequencies of which the values are of the same order of magnitude as those of the modes in which only the lithium and only the fluorine nuclei respectively oscillate. These considerations enable us to arrange the nine modes of free vibration of the structure in a descending order

Table 1. Description of the normal modes

Mode	Description	Degeneracy	Frequency
I	Oscillation of the lithium and fluorine nuclei in opposite phases	3	ν_1
II	Oscillation of the lithium nuclei in the octahedral planes normally	4	ν_2
III	Oscillation of the lithium nuclei in the octahedral planes tangentially	8	ν_3
IV	Oscillation of the lithium and fluorine nuclei in the cubic layers tangentially	6	ν_4
V	Oscillation of the lithium and fluorine nuclei in the cubic layers normally	3	ν_5
VI	Oscillation of the fluorine nuclei in the octahedral planes normally	4	ν_6
VII	Oscillation of the fluorine nuclei in the octahedral planes tangentially	8	ν_7
VIII	Oscillation of the lithium and fluorine nuclei in the cubic layers normally	3	ν_8
IX	Oscillation of the lithium and fluorine nuclei in the cubic layers tangentially	6	ν_9
	Translations	3	$\nu_9 \rightarrow 0$
	Total	48	—

of frequency as shown in table 1. On a comparison with the tables of the same kind appearing in the memoirs on MgO and NaCl referred to above, it will be seen that many features are common to all the three cases, a rearrangement appearing only in respect of the modes located near the middle of the table. The principal differences between the three cases are in respect of the relative magnitudes of the various frequencies. In the cases of MgO and NaCl, the frequencies are distributed pretty evenly in their values between the highest and the lowest. In the case of lithium fluoride, on the other hand, four of the frequencies form a group with higher values and the four others form another group with lower values.

In the memoir dealing with the case of magnesium oxide, the dynamical theory which gives explicit formulae for the nine vibration frequencies was developed both in the first and second approximations. Very simple relations between the frequencies ν_1, ν_2, ν_3, ν_6 and ν_7 appear in the first approximation. They are also valid in the second approximation, if we consider only the interactions between each atom of one species and its neighbours of the other species. These relations are, $\nu_1 = k/\mu$, $\nu_2 = \nu_3 = k/m_1$, $\nu_6 = \nu_7 = k/m_2$, where m_1, m_2 are the masses of the two species of atoms, μ is the reduced mass given by the relation $1/\mu = 1/m_1 + 1/m_2$ and k is the operative force-constant. As will be shown later in this memoir, the infra-red absorption studies with lithium fluoride enable a very

precise determination to be made of the highest vibrational frequency ν_1. This comes out as 508 cm^{-1} in wave-numbers. From this and the foregoing relations, we obtain $\nu_2 = \nu_3 = 435\,cm^{-1}$ and $\nu_6 = \nu_7 = 263\,cm^{-1}$. There are good reasons for assuming that the interaction between each atom and the atoms of the same species surrounding it in the structure of lithium fluoride can be neglected in comparison with the interactions between the atoms of different species. This assumption is equivalent to assuming that the difference between ν_2 and ν_3 and the difference between ν_6 and ν_7 are both unimportant. Since ν_1 is precisely determined, the values for ν_2, ν_3, ν_6 and ν_7 thus calculated can be confidently made use in the evaluation of the thermal energy content. These five frequencies between them account for 27 out of the total of 48 degrees of dynamic freedom. The remaining four frequencies ν_4, ν_5, ν_8 and ν_9 which between them carry 18 degrees of freedom are, as we shall presently see, accessible to observation by infra-red absorption studies.

4. The origin of infra-red activity

As has been stated earlier, the spectrum of free vibrations of the crystal exhibits the frequencies of oscillation of its atomic nuclei about their positions of equilibrium. In determining these frequencies, the massive positively charged atomic nuclei play the major role, while the negatively charged electrons play the subordinate role of holding the nuclei in their positions of equilibrium and of setting up the forces which return the nuclei to those positions when disturbed therefrom.

The spectrum of infra-red absorption and the spectrum of free vibrations are fundamentally different in their nature and origin and cannot therefore be identified with each other. This becomes clear when it is remarked that infra-red absorption represents a transfer of energy from the field of the radiation to the substance of the crystal. For such a transfer to be possible, the field should give rise to a periodic displacement of the mobile electrons present in the structural units of the crystal. This displacement would, on the one hand, excite the vibrations of the structural units and would on the other hand react on the field of radiation and cause its extinction. In these processes, the electrons clearly play the leading role and the atomic nuclei only a subordinate one, thus reversing the position which obtains in the case of the free vibrations.

It is evident that if we assume each nucleus in the structure to carry with it in its movements the full quota of electrons required to neutralise its positive charge, the crystal could display no infra-red activity. It follows that the negative charges of which the movements are the effective cause of infra-red absorption are the electrons which hold the different nuclei together and hence do not participate fully in the movements of any particular nucleus. The movements of these electrons would evidently be determined by the symmetry of their situation and

the symmetry of the movements of the nuclei between which they are located. Lack of such symmetry is clearly indicated as a necessary condition for their being set in motion by the field of the incident radiation and for the excitation of the nuclear vibrations resulting in the transfer of energy from the field to the crystal.

5. Activity of the normal modes

Since the crystal structure of lithium fluoride resembles those of magnesium oxide and of rock-salt, the considerations already set out fully in the two earlier memoirs regarding the infra-red activity of the different normal modes would be applicable also in the case of lithium fluoride. As has already been remarked, however, the case of lithium fluoride presents exceptional features, in particular a great disparity in the atomic weights of the two species of nuclei present in its structure. This disparity carries with it a corresponding disparity in the charges carried by the nuclei. Noteworthy differences in infra-red behaviour stemming from these factors are therefore to be expected. We may usefully here make a comparison between the cases of LiF, MgO and NaCl.

The reduced mass of the nuclei appearing in the formulae for the frequencies of vibration are respectively in these three cases, 5·08, 9·65 and 13·97. Lithium fluoride resembles magnesium oxide in its low solubility in water. Their crystal spacings are not also very different, being 4·01 and 4·203 Å respectively. In these circumstances and since magnesium is divalent whereas lithium is monovalent, the bonding forces in MgO may be presumed to be about twice as strong as in LiF. It follows that the highest vibration frequency would be roughly about the same for lithium fluoride as for magnesium oxide. This indeed, as we shall see, is actually the case. On the other hand, in the case of NaCl, the corresponding frequency is far too low to be accounted for as due solely to the increased mass. The much weaker binding indicated by its solubility in water and the larger crystal spacing has also to be considered.

While the infra-red behaviour of MgO and LiF may thus be similar in some respects, noteworthy differences are also to be expected in view of the factors already alluded to, viz., the great disparity in the masses and charges of the two species of nuclei in the case of lithium fluoride. The disparity in masses would lead to marked differences in the distribution of frequencies in the spectrum. The disparity in the nuclear charges may likewise be expected to result in marked differences in the activities of the different modes, both absolutely and relatively to each other. We may therefore proceed to recall here briefly the behaviour of the different modes in their qualitative aspects as deduced in the earlier memoirs.

The mode of highest frequency in which the lithium and fluorine nuclei oscillate with respect to each other would necessarily be infra-red active, both in the first-order and in the higher orders. In other words, besides the absorption of radiations having nearly the same frequency, we should also expect absorptions

to appear in the regions where the frequency is nearly twice or thrice or four times the frequency of that mode, the strength of such absorption diminishing rapidly with increasing order. Taking the highest frequency in wave-numbers as 508 cm^{-1} and the corresponding wavelength as 19·68 μ, we should expect the absorption of the second-order to appear at 9·84 μ, the absorption of the third-order at about 6·6 μ, and the fourth-order at 4·9 μ. We shall see later that these indications of the theory find support in the observed behaviour of lithium fluoride.

The octahedral modes of vibration listed as II, III, VI and VII in table 1 would be infra-red inactive both in the first and in the higher approximations by reason of the symmetry which they possess, as has already been explained fully in the earlier memoirs. On the other hand, the cubic modes of vibration listed as IV, V, VIII and IX in table 1, though inactive in the first approximation, would be active in the higher approximations. In particular, they may be expected to manifest themselves strongly with doubled frequencies in the infra-red absorption spectrum.

6. Methods of investigation

Following the same procedure as that adopted for magnesium oxide, the infra-red transmission curves of lithium fluoride were recorded using a Leitz spectrophotometer provided with NaCl optics for the spectral range between 1 μ and 15 μ and KBr optics for the range between 13 μ and 24 μ. A clear transparent block of lithium fluoride of 1·8 cm × 1·8 cm cross-section was available. From this, a whole series of plates could be obtained by cleavage of different thicknesses. But the optical performance of plates obtained by simple cleavage was not always satisfactory. Hence, it was found to be a better procedure first to obtain a plate of nearly the desired thickness by cleavage and then by grinding and polishing to give its faces a satisfactory finish. In this fashion, it was found possible to carry the investigation down to thicknesses as small as a tenth of a millimetre. The fragility of the material prevents obtaining still thinner plates of adequate size.

The absorption and reflection are both so large at wavelengths greater than 15 μ that the technique described above then ceases to be inapplicable. Two other procedures analogous to those employed in the case of MgO were accordingly followed. One was to stir very finely ground lithium fluoride into liquid paraffin and to study the transmission by a thin film of the mixture held between KBr plates, balancing it against a similar film of paraffin alone. The second method was to mix a very small quantity of finely divided lithium fluoride with KBr powder and press the mixture in vaccum under high pressure into a flat tablet, the transmission by which was investigated.

Some sixty records in all were made with thirty different absorption paths at fairly close intervals, so as to reveal clearly how the strength of the absorption

varied with the wavelength over the entire spectral range under consideration. The majority of the records were obtained with absorption paths less than one millimetre, for it is in this range, as in the case of magnesium oxide, that the most interesting changes appear in the character of the transmission curves. Nine records out of the large number made are reproduced with this memoir, the selection being made with a view to illustrate the most significant features revealed by the studies.

7. The experimental results

We shall set out the results of the studies by dividing the spectral range covered by them into five different sectors and describing the behaviour of the transmission in these sectors as recorded with different absorbing thicknesses.

I. 4μ *to* 5μ.—With the maximum thickness employed in these studies, viz., 1·8 cm, the transparency is complete in the wavelength between 1μ and 4μ. But between 4μ and 5μ, the transmission falls by about 5%. But this effect ceases to be observable when the thickness of the plate is five millimetres or less, the curve then running quite horizontally between these wavelengths. It is evident that the absorption between 4μ and 5μ is extremely weak.

II. 5μ *to* 8μ.—With an absorption path of 1·8 cm the transmission which is 92% at 5μ falls steeply at greater wavelengths, reaching a value of only 18% at $6{\cdot}5\mu$. Beyond this wavelength, the decrease becomes less rapid. The transmission

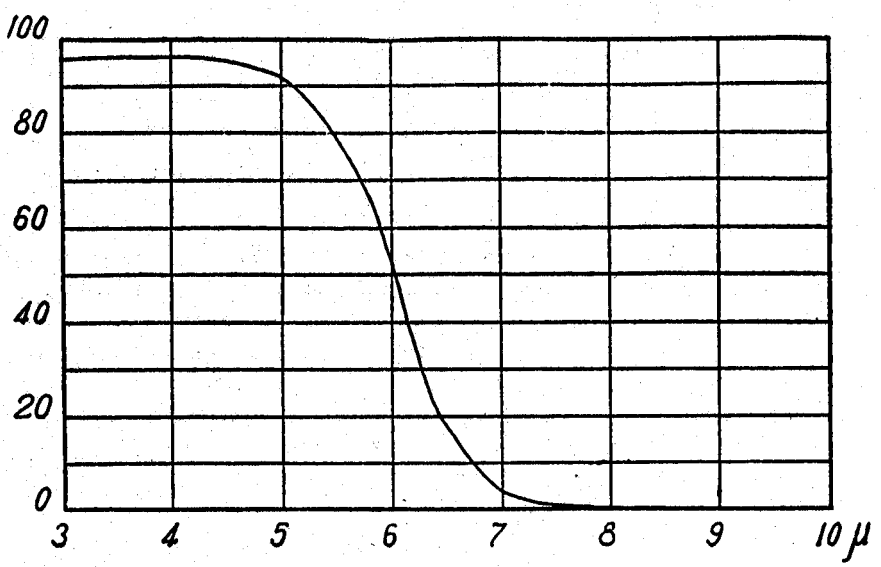

Figure 1. Transmission percentages of block 1·8 centimetres thick.

goes down to 4% at 7 μ and is practically zero at 7·5 μ. At 8 μ and all greater wavelengths there is a complete cut-off. These features are evident in the record reproduced as figure 1 in the text.

When the thickness of the plate traversed by the radiation is reduced from a centimetre or more to a few millimetres, the wavelength at which a cut-off appears moves to 10 μ, a sensible transmission then appearing in the region between 8 μ and 10 μ. These features are noticeable when the absorption path is five millimetres and become increasingly more conspicuous as the thickness is further reduced.

The record of the percentage transmission by a plate 2·92 millimetres thick is reproduced as figure 2 in the text and illustrates the remarks made above. The

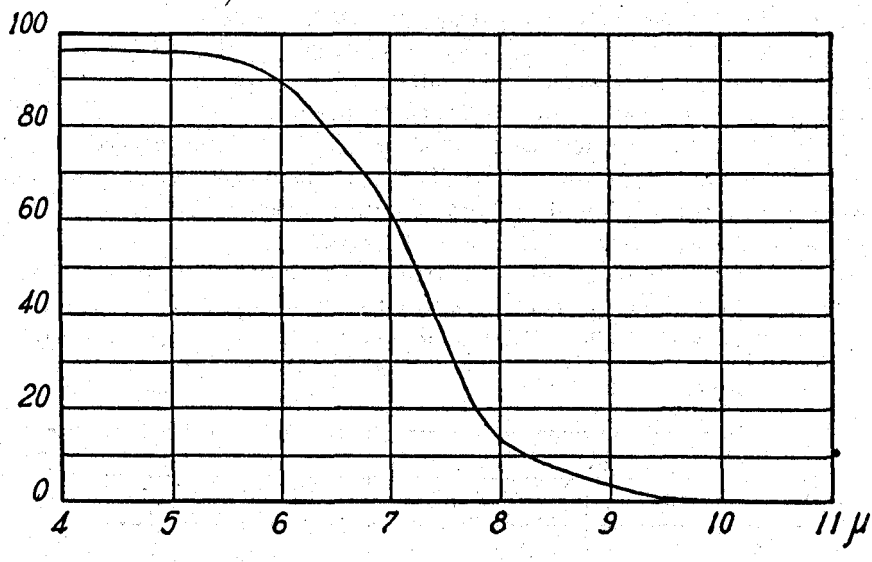

Figure 2. Percentage transmission by plate 2·92 millimetres thick.

curve may be described as consisting of five distinct sectors, viz., a part between 4 μ and 5 μ where it runs horizontally, a part between 5 μ and 6 μ where is a gentle fall, then a rapid fall between 6 μ and 7 μ, a fourth part between 7 μ and 8 μ where the fall is even more rapid with an inflexion at 7·6 μ and finally a gentle slope between 8 μ and the cut-off at 10 μ.

A comparison of figure 1 with figure 2 shows that the transmission at all wavelengths has notably increased in the latter. The transmission at 6 μ has improved from 52% to 90%. The transmission at 7 μ has increased from 4% to 62% and that at 8 μ from 0% to 13%.

III. 8 μ *to* 10 μ.—The record of the transmission appearing in this sector when the cut-off has shifted from 8 μ to 10 μ initially exhibits a concavity upwards. As

the thickness diminishes, the transmission at 8 μ improves rapidly. It is zero for an absorption path of 1·8 centimetres, 12% for a thickness of 2·8 millimetres and 50% for a thickness of one millimetre. The slope of the graph between 8 μ and 10 μ increases rapidly in consequence and its shape alters at the same time. Its curvature diminishes and the graph appears as a nearly straight line with fairly sharp bends near its two extremities. With smaller thicknesses, the graph is curved in the opposite sense with its convexity directed outwards. But at this stage the cut-off at 10 μ has disappeared and an appreciable transmission appears beyond that wavelength.

A remarkable series of changes in the form of the transmission curve between 8 μ and 10 μ is recorded when the thickness of the plate is progressively reduced from one millimetre down to a tenth of a millimetre. They are depicted in figures 3, 4, 5, 6, 7 and 8. The graph between 8 μ and 10 μ does not run continuously into that of the next sector between 10 μ and 15 μ. Intervening between them appears an arrest or horizontal strip located between 9·8 μ and 10 μ. As the thickness is progressively reduced, this feature retains its position on the scale of wavelengths but moves upwards. When the thickness is reduced below 0·4 millimetres, it changes its character and develops into a V-shaped depression. This becomes increasingly more conspicuous as the thickness is reduced, and the tip of the depression then appears as a sharp point.

IV. 10 μ *to* 15 μ.—The changes appearing in this sector as the absorption thickness is diminished are depicted in figures 3, 4, 5, 6, 7 and 8. When the thickness

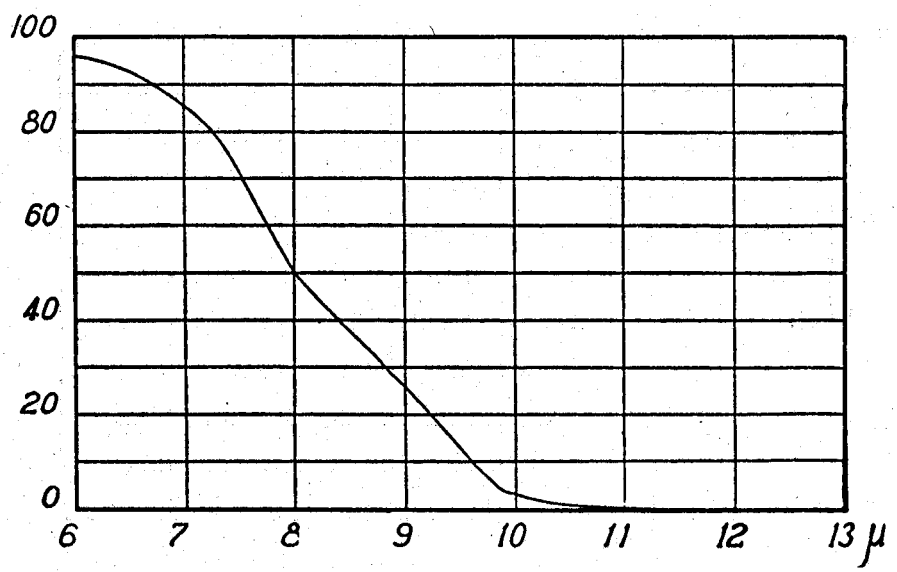

Figure 3. Percentage transmission by plate 1 millimetre thick.

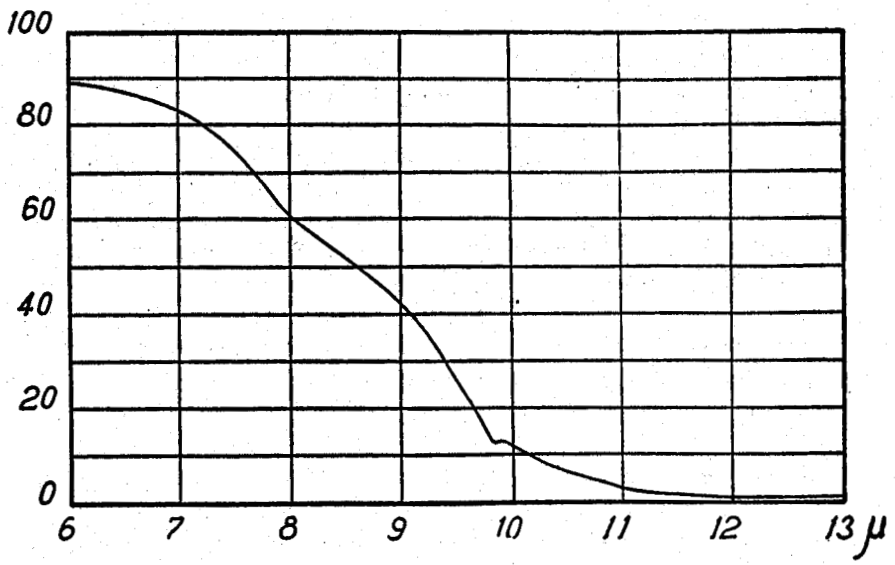

Figure 4. Percentage transmission by plate 0·6 millimetre thick.

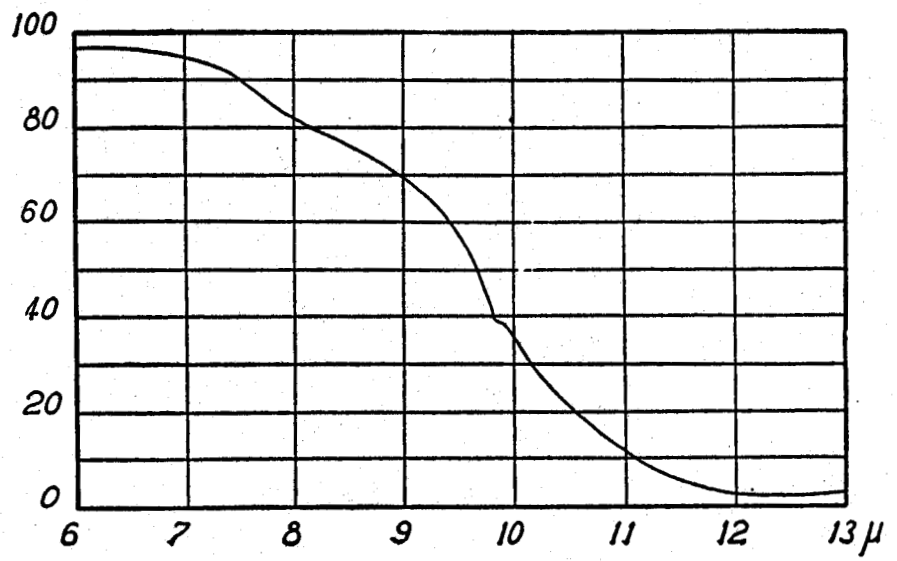

Figure 5. Percentage transmission by plate 0·4 millimetre thick.

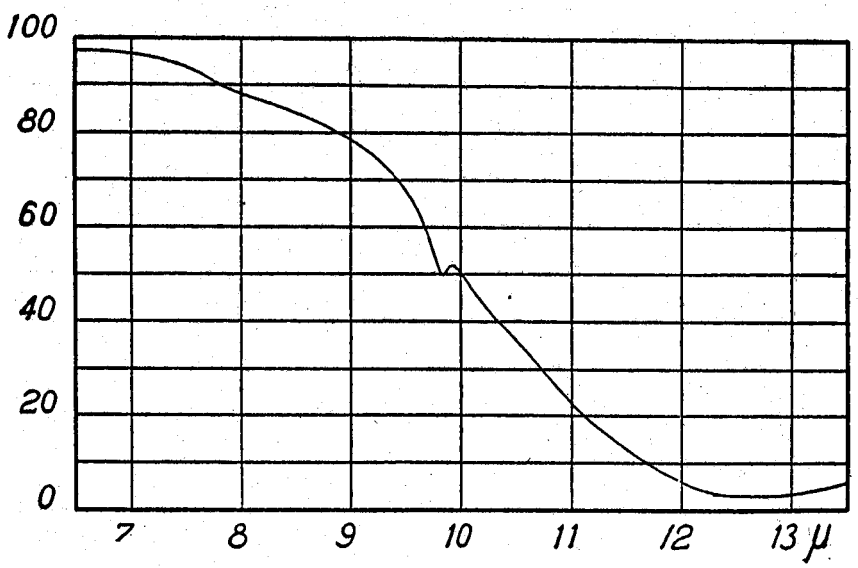

Figure 6. Percentage transmission by plate 0·34 millimetre thick.

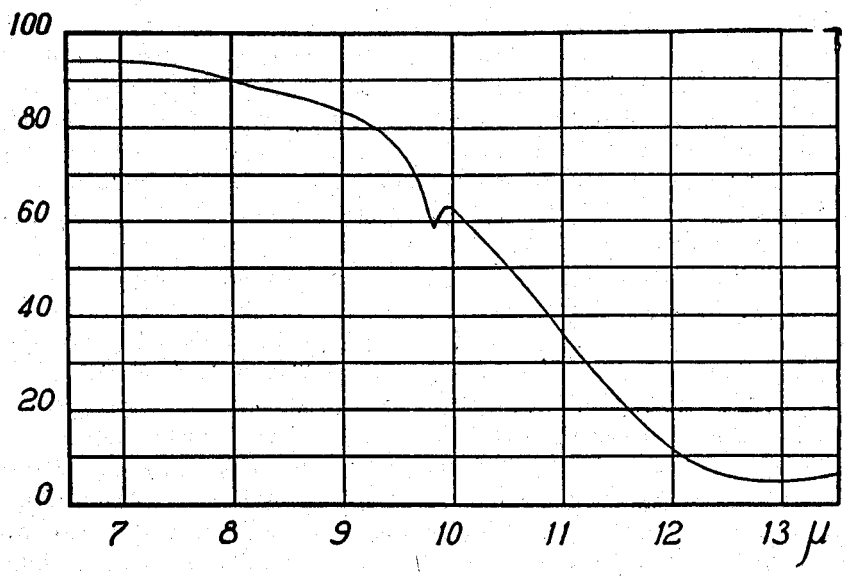

Figure 7. Percentage transmission by plate 0·18 millimetre thick.

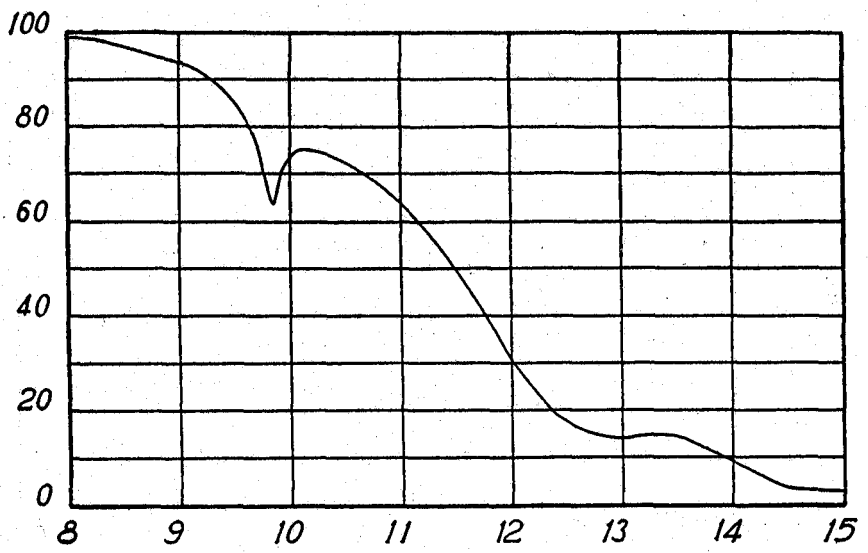

Figure 8. Percentage transmission by plate 0·10 millimetre thick.

is reduced from 2·92 millimetres to 1 millimetre, the cut-off at 10 μ moves to 11 μ and when it is further reduced the cut-off disappears and a weak transmission is noticed extending up to 13 μ and even beyond 13 μ. With a thickness of 0·4 millimetre, the wavelength at which the percentage transmission is least may be placed at 12 μ. As the thickness is further reduced and the transmission improves, the wavelength at which the transmission is a minimum moves towards longer wavelengths and finally reaches 13 μ with the thinnest plates. Beyond 13 μ, the transmission is distinctly larger and shows a distinct maximum at about 13·4 μ. It then falls off to a much smaller value at 15 μ which is the end of the range of the spectrograph with NaCl optics. Records obtained with KBr optics using the thinnest obtainable plates show a transmission of 14% at 13 μ, rising to 15% at 13·5 μ, and then falling to 12% at 14 μ and going down smoothly to zero at 15 μ. Beyond 15% there is a complete cut-off.

V. 15 μ *to* 24 μ.—In this range which is accessible to study using KBr optics in the spectrograph, six records were obtained exhibiting the transmission by very small absorption paths in lithium fluoride. Three of these records were made by the pellet technique, three different quantities of finely powdered lithium fluoride, 1 milligram, 0·5 milligram and 0·25 milligram respectively being incorporated with one gram of KBr and pressed into a flat circular tablet the transmission by which was investigated. Three records were also made of the transmission by a layer of liquid paraffin and very finely divided lithium fluoride made up into a paste. One of the records was made with a spacer separating the plates between

which the paste was held. The other two records were made without a spacer but with different quantities of the lithium fluoride in the paste.

The record made by the paste technique with a spacer 30 μ thick resembled those obtained with the thinnest plates but with the cut-off appearing at 18 μ instead of at 15 μ. When there was no spacer and the effective thickness of the film was therefore extremely small, a transmission appeared over the entire spectral range. But it was much greater between 13 μ and 16 μ than between 18 μ and 24 μ, a transition appearing between 16 μ and 18 μ.

The results obtained with the pellet technique are qualitatively similar but quantitatively different with the three different quantities of the lithium fluoride. A large transmission appears between 13 μ and 16 μ and a notably smaller transmission between 18 μ and 24 μ, with a region of transition between 16 μ and 18 μ. The record made with the half-milligram of lithium fluoride in the pellet is reproduced as figure 9. It exhibits five different features, (*a*) a region of nearly complete transparency between 13 μ and 15·5 μ, (*b*) a region of diminishing transparency between 15·5 μ and 18 μ, (*c*) a region of constant transparency between 18 μ and 20 μ, (*d*) a region of diminishing transparency between 20 μ and 22 μ, and finally, a region of nearly constant transparency between 22 μ and 24 μ.

8. Significance of the results

The most important result which emerges from the present studies is that a sharply-defined minimum of transmission appears at 9·84 μ. This is most strikingly exhibited in figure 8. Its origin is evident from the circumstances in which it is observed. It can indisputably be identified as the second-order absorption due to the mode of vibration listed as having the highest frequency ν_1 in table 1, in other words, the oscillation of the lithium and fluorine nuclei in opposite phases. The wavelength 9·84 μ corresponds to double this frequency or $2\nu_1$. The sharpness with which it is recorded is an objective demonstration that this free vibration possesses a definite monochromatic frequency.

The frequency ν_1 corresponds to a wavelength 19·68 μ which is double 9·84 μ. Since the vibrational mode of that frequency is active not only in the first-order but also in the higher orders, we should expect to find evidence of such activity in the appropriate regions of the spectrum, viz., around 6·6 μ in the third-order, around 4·9 μ in the fourth-order and around 3·9 μ in the fifth-order respectively the strength of such activity falling off rapidly with increasing order. This agrees with the recorded results of experiment. The absorption of the fifth-order to be expected at 3·9 μ is too weak to be recorded with a thickness of 1·8 cm. But there is an observable absorption at 4·9 μ with that thickness. This, however, disappears when the thickness is reduces to 5 millimetres. On the other hand, the records for various thicknesses exceeding one millimetre all exhibit the third-order absorption at 6·6 μ. The strength of this absorption becomes progressively less

conspicuous as is indicated by the steepness of the fall of the transmission percentage at that wavelength. It finally ceases to be noticeable when the thickness is one millimetre or less. But at these same thicknesses the second-order absorption at 9·84 μ is conspicuous and continues to be observable even with the thinnest obtainable plates. It is thereby made evident that the second-order absorption is far more powerful than the third-order effect.

Referring to table 1, we find in it listed as modes IV and V with the frequencies ν_4 and ν_5 the coupled vibrations of the lithium and fluorine appearing in the cubic layers. These two modes are inactive in the first-order but active in all higher orders. From a study of the transmission curves reproduced in the present memoir, we are enabled to recognise the activity of these two modes and locate their characteristic wavelengths at 24 μ and 26 μ respectively. We should accordingly expect them to give rise to readily observable third-order absorptions as 8 μ and 8·7 μ respectively and to powerful second-order absorptions at 12 μ and 13 μ. These absorptions are easily recognisable in the series of figures reproduced above in the text. Indeed, it is clear that these two vibrational modes contribute in a very large measure to the features noticeable in the spectroscopic records of transmission percentage.

We have now to ascertain the frequencies ν_8 and ν_9 of the two other modes of coupled vibration of the lithium and fluorine nuclei appearing in the cubic layers and listed as VIII and IX in table 1. If we take $\nu_8 \approx \nu_9 = 210\,\text{cm}^{-1}$ in wavenumbers, the corresponding wavelength would be 47·6 μ. The second-order absorption due to this would appear at 23·8 μ. That this is the wavelength at which the minimum transmission appears in figure 9 may be regarded as a justification for the assumed values of ν_8 and ν_9. Thus, finally, we have in table 2 a list of the nine modes of free vibration of the lithium fluoride structure, their degeneracies, their frequencies and their characteristic wavelengths.

Table 2. Modes and frequencies

Mode	Degeneracy	Frequency cm^{-1}	Wavelength μ
I	3	$\nu_1 = 508$	19·68
II	4	$\nu_2 \approx 435$	23
III	8	$\nu_3 \approx 435$	23
IV	6	$\nu_4 = 417$	24
V	3	$\nu_5 = 384$	26
VI	4	$\nu_6 \approx 263$	38
VII	8	$\nu_7 \approx 263$	38
VIII	3	$\nu_8 \approx 210$	48
IX	6	$\nu_9 \approx 210$	48
Translations	3	$210 \rightarrow 0$	$48 \rightarrow \infty$
Total	48	—	—

9. The rest-strahlen reflections

According to Czerny and Roder (*Ergebn-exakt. Naturwiss.*, **17**, 70 (1938)), the reflecting power of a lithium fluoride surface is quite small at 12 μ and only 20% at 14 μ. It rises steeply to 62% at 15 μ and thereafter goes up less abruptly to a maximum of 75% at 18 μ. Beyond this again, it dips a little to 72% at 20 μ and rises to a second maximum of 92% at 26 μ. It then falls off progressively. It is 86% at 30 μ, 68% at 35μ, 35% at 40 μ and 28% at 50 μ.

These facts of observation become intelligible when considered in relation to the spectroscopic behaviour of lithium fluoride as elucidated in the present memoir. It is evident from the investigation that the second-order absorptions due to the coupled vibrations in the cubic layers are very powerful. Indeed, from figure 9 it is evident that the second-order activity of modes VIII and IX is actually greater than the first-order activity of mode I. It is therefore to be expected that the reflecting power at 20 μ, though large, would be less than that at greater wavelengths. The appearance of a second and more pronounced maximum at 26 μ is this explained.

The slow drop of the reflecting power with increasing wavelength beyond 26 μ is clearly the result of the co-operation of all the nine modes of free vibration of the structure. Technically, all these modes except the first are infra-red inactive. But this is only in the first approximation. The intense excitation near the surface of the crystal due to the active modes and overtones would necessarily also involve the excitation of all other modes to a greater or less extent determined by the differences between their frequencies and those of the active modes. It follows that

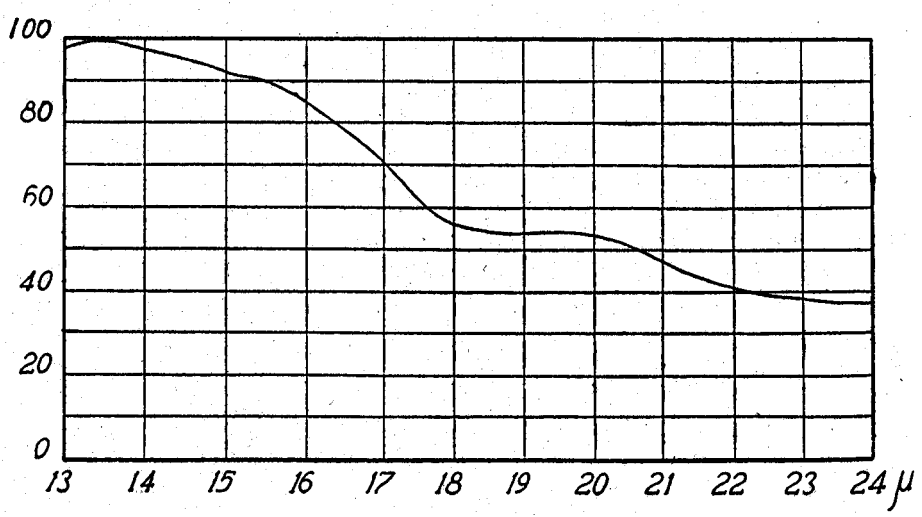

Figure 9. Record of transmission obtained with the pellet technique.

enhanced reflecting power should extend, though with progressively diminishing strength, over the entire range of wavelengths listed in table 2.

10. Computation of the atomic heats

The details of the procedure adopted for the evaluation of the thermal energy of the crystal have already been set out fully in the earlier memoirs dealing with the cases of MgO, NaCl and diamond. It is therefore unnecessary to traverse the same ground here. The unit oscillators with the total of whose energies of vibration we identify the heat content are the 16-atom groups composed of 8 lithium atoms and 8 fluorine atoms. Of the total of 48 degrees of freedom of each such group, 45 degrees of freedom are identified with the modes of their internal vibration, while the 3 remaining degrees of freedom represent their translational movements. These latter again may be identified with the internal vibrations in volume elements of larger size, the frequencies of which diminish as the linear dimensions of the volume elements increase. The number of such volume elements present in the crystal varies inversely as the cube of their linear dimensions. The contribution of these vibrations to the thermal energy content would therefore fall off rapidly as their frequencies go down. The same can be evaluated on the basis of Einstein's theory, except that instead of a summation over a discrete set of frequencies, it appears as an integration based on the distribution law $3N \cdot 3\nu^2 d\nu$ derived on the basis of the foregoing considerations, where N represents the number of 16-atom groups contained in the crystal.

Table 3 sets out the computations made for the lower and most interesting part of the temperature range in which the atomic heat goes up rapidly from zero to fairly high values. Table 4 exhibits the computations in the higher range of temperatures up to 500° K. The theoretical calculations are based upon the assumption that the oscillators are harmonic. They also ignore the changes in the frequencies of vibration which accompany the changes in temperature and are related to the thermal expansion of the crystal.

The experimental data have been shown in table 5 for the lower range of temperature and in table 6 for the higher range. The references to the original literature from which the experimental data have been taken have been entered below the respective tables. The specific heats as actually measured are the values at constant pressure. At low temperatures, they do not differ sensibly from the specific heats at constant volume. But it is the latter which can appropriately be compared with the theoretically determined values. Hence it is necessary to compute the specific heats at constant volume from those at constant pressure as experimentally determined. The corrections involve a knowledge of the thermal expansion co-efficient of the crystal and of its isothermal compressibility at the various temperatures.

The thermal expansion of lithium fluoride has been measured over a wide

Table 3. Computation of the atomic heats of LiF

	20° K	40° K	60° K	80° K	100° K	120° K	140° K	160° K	180° K	200° K	220° K	240° K	260° K
$3E_1(508)$	—	—	0·0003	0·0030	0·0124	0·0295	0·0530	0·0794	0·1061	0·1318	0·1559	0·1775	0·1971
$12E_2(435)$	—	0·0001	0·0042	0·0338	0·1054	0·2121	0·3368	0·4604	0·5773	0·6850	0·7784	0·8589	0·9275
$6E_3(417)$	—	—	0·0030	0·0215	0·0633	0·1218	0·1868	0·2518	0·3104	0·3630	0·4074	0·4482	0·4811
$3E_4(384)$	—	0·0001	0·0028	0·0166	0·0435	0·0775	0·1133	0·1464	0·1760	0·2012	0·2224	0·2414	0·2568
$12E_5(263)$	—	0·0094	0·1025	0·2870	0·4932	0·6755	0·8250	0·9413	1·0342	1·1053	1·1642	1·2085	1·2449
$9E_6(210)$	0·0001	0·0309	0·1782	0·3718	0·5398	0·6672	0·7603	0·8315	0·8828	0·9224	0·9533	0·9759	0·9948
3D(210)	0·0081	0·0574	0·1325	0·1969	0·2430	0·2747	0·2966	0·3124	0·3236	0·3321	0·3387	0·3435	0·3476
Atomic heat	0·0082	0·0979	0·4235	0·9306	1·5006	2·0583	2·5718	3·0232	3·4104	3·7408	4·0203	4·2539	4·4498

Table 4. Computation of the atomic heats of LiF

	280° K	300° K	325° K	350° K	375° K	400° K	425° K	450° K	475° K	500° K
$3E_1(508)$	0·2139	0·2293	0·2457	0·2594	0·2713	0·2821	0·2911	0·2982	0·3052	0·3112
$12E_2(435)$	0·9863	1·0377	1·0953	1·1417	1·1802	1·2116	1·2419	1·2653	1·2852	1·3036
$6E_3(417)$	0·5103	0·5342	0·5610	0·5821	0·6011	0·6165	0·6297	0·6412	0·6506	0·6578
$3E_4(384)$	0·2696	0·2805	0·2927	0·3021	0·3105	0·3171	0·3227	0·3277	0·3316	0·3362
$12E_5(263)$	1·2767	1·3013	1·3264	1·3508	1·3672	1·3798	1·3925	1·4025	1·4105	1·4178
$9E_6(210)$	1·0146	1·0254	1·0380	1·0474	1·0564	1·0633	1·0699	1·0748	1·0795	1·0830
3D(210)	0·3511	0·3536	0·3563	0·3582	0·3600	0·3614	0·3628	0·3638	0·3647	0·3655
Atomic heat	4·6225	4·7620	4·9154	5·0417	5·1467	5·2318	5·3106	5·3735	5·4273	5·4751

Table 5. Comparison of the experimental and theoretical values of the atomic heats (C_v) of LiF

Temperature	20° K	40° K	60° K	80° K	100° K	120° K	140° K	160° K	180° K	200° K	220° K	240° K	260° K
Interpolated experimental values	0·0086	0·1030	0·4110	0·9340	1·5250	2·1270	2·6650	3·1220	3·5080	3·8150	4·0760	4·2840	4·4580
Calculated values	0·0082	0·0979	0·4235	0·9306	1·5006	2·0583	2·5718	3·0232	3·4104	3·7408	4·0203	4·2539	4·4498

Experimental values of the atomic heats of LiF from K Clusins, J Goldmann and A Perliek, *Z. Naturforsch.*, A4, 424–432 (1949).

Table 6. Comparison of the experimental and theoretical values of the atomic heats of LiF

Temperature	300° K	325° K	350° K	375° K	400° K	425° K	450° K	475° K	500° K
Experimental values of C_p	5·0210	5·1885	5·3335	5·4595	5·5710	5·6705	5·7600	5·8410	5·9155
Corrected for C_v	4·7724	4·9110	5·0245	5·1165	5·1908	5·2500	5·2951	5·3281	5·3496
Calculated values	4·7620	4·9154	5·0417	5·1467	5·2318	5·3106	5·3735	5·4273	5·4751

Experimental values of the atomic heats of LiF from T B Douglas and J L Dever, *J. Am. Chem. Soc.* **76**, 4826 (1954).

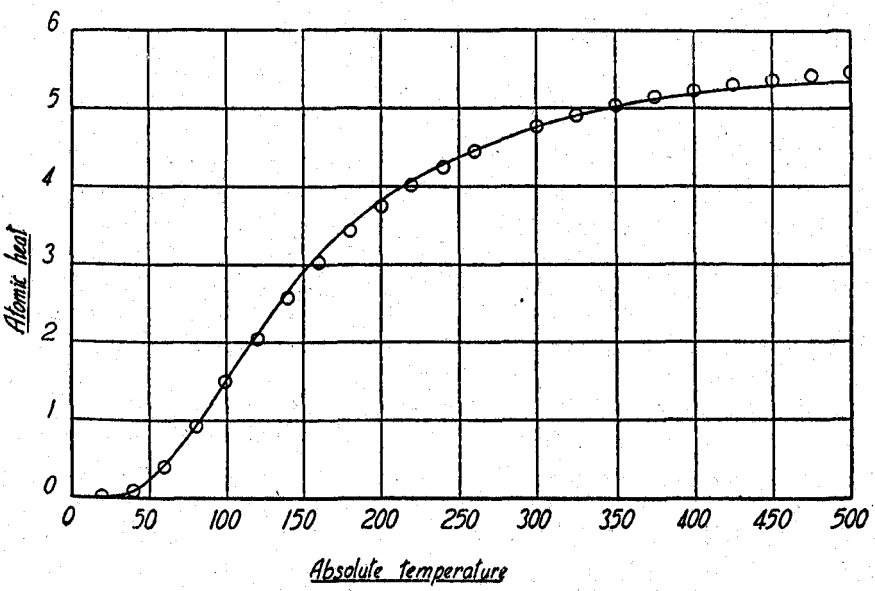

Figure 10. Comparison of the theoretically calculated and experimentally determined atomic heats. Experimental results———; theoretical values ○○○○.

range of temperatures. The compressibility, however, has only been determined near room temperatures. Some uncertainty is thereby introduced in effecting the reduction from C_p to C_v.

Tables 5 and 6 show a satisfactory over-all agreement between the theoretically computed and experimentally determined values of atomic heat over the entire range of temperature from absolute zero up to 500° K. This agreement is graphically exhibited in figure 10.

Summary

The records of the transmission percentages of infra-red radiation by thin plates of lithium fluoride enable the frequency of the vibration of the lithium and fluorine nuclei against each other in opposite phases to be precisely determined. The frequencies of the four inactive modes can be computed therefrom. Four other modes are active as overtones and their frequencies can be directly determined from the records. A theoretical computation of the specific heat of lithium fluoride on the basis of the spectroscopic data alone thus becomes possible. A very satisfactory agreement emerges between the theoretically computed and experimentally determined values of the atomic heats of the crystal over the entire range of temperatures from absolute zero to 500° K.